Generation of Drops and Satellites by Two Mode EHD Stimulation of a Continuous Jet

B. Barbet*†, P. Atten† and A. Soucemarianadin*‡
****TOXOT Science & Applications, Groupe IMAJE, Cedex, France***
†L.E.M.D.—CNRS & Univ. J. Fourier, Cedex, France
‡Laboratoire de Rhéologie—CNRS & Univ. J. Fourier, Cedex, France

Abstract

This paper presents experiments performed on a scaled-up electrohydrodynamic jet stimulation device. The investigation considers particularly the introduction of the second harmonic in the excitation signals. The excitation frequency, the amplitude and phase of the signals are independently controlled leading to a variety of drop break-up patterns. The most suitable conditions for printer applications are emphasized.

Introduction

Continuous ink-jet technology requires the formation of drops, from a jet, at a well-defined rate. On one hand, piezoelectric stimulation producing velocity disturbances which grow through surface tension forces until the jet breaks up into uniform drops has been used[1]. Although this type of stimulation may allow the formation of a stream of drops devoid of satellites, it presents the noticeable disadvantage of acoustic crosstalk when operated in multijet devices[2]. On the other hand, the use of ElectroHydroDynamic (EHD) exciters[3,4] which are easier to design because the excitation is downstream the nozzle could be preferable in multijet printers. A well known limitation of this type of excitation is the occurrence of secondary droplets or so called satellites which are deleterious for appropriate printing since they lead to drop placement errors in the final image. It has been shown both in the case of acoustic and EHD exciters[5,6] that the formation of satellite-droplets is controlled by interactions between the harmonics of the fundamental excitation. The harmonics could either arise because of non linear fluid mechanical effects related to the excitation mode and/or nozzle effects[7], or be introduced purposely into the jet by the EHD exciters[6].

In this paper, following Rezanka and Crowley[6], we present results on the EHD stimulation of a continuous jet using two modes of frequency f and $2f$. More particularly, we have performed experiments with various electrode configurations at different wavenumbers, using a well characterized fluid. Section II details our scaled-up drop generation set-up, which has been used previously both for multi-electrode continuous EHD stimulation[4] and for pulsed EHD excitation[8]. Section III contains a discussion of the different regimes of breakup obtained, depending on the ratio and phase shift between the two modes. Section IV presents selected results for the operating conditions which allow or suppress the formation of satellites. Finally section V summarizes the main conclusions.

Originally published in *Proc. of IS&T's Eleventh International Congress on Advances in Non-Impact Printing Technologies*, October 29-November 3, 1995 in Hilton Head, South Carolina.

Experimental Arrangement and Procedures

The experimental set-up is shown in Figure 1. The jet ($2a$ = 0.44 mm in diameter) emerges from a 12 mm long hypodermic needle. The jet velocity ($U_o \cong 5$ m/s) is carefully controlled by means of a pressure regulated tank containing the fluid. The stimulation electrodes located at a distance of about 3.2 mm downstream from the nozzle consist of a set of five steel rods (rod diameter: 0.7 mm; pitch: 2.25 mm). Electrodes 1, 3 and 5 are grounded (Figure 1). The signal applied to electrode 2 is at frequency $f \cong 850$ Hz whilst that of electrode 4 is at frequency $2f$. We choose to work at a dimensionless wavenumber $k = (2\pi a/\lambda) < 0.5$ (λ is the wavelength) in order to amplify the second harmonic. In contrast to Rezanka and Crowley[6] we are able to stimulate the jet with simple sinusoids. Moreover with our electrode configuration, we are not limited in the order of the harmonic which can be introduced into the jet. The two different waveforms of the driving voltages are simultaneously synthesized using software. The digital signals are first converted to analog ones and used to drive two high voltage amplifiers with peak to peak amplitudes as high as 1.2 kV. The output from the amplifiers have the following form:

$$V_1(t) = V_1 \cos(\pi f t) \text{ and } V_2(t) = V_2 \cos(2\pi f t + \frac{\phi}{2}) \qquad (1)$$

The electrostatic pressures $P_i(t)$ (attractive force on the surface of the jet) are proportional to $V_i^2(t)$. The disturbances applied onto the jet are the fundamental for the first electrode and the second harmonic for the elec-

trode located downstream. This introduces a spatial phase shift depending on both the jet velocity U_o and the distance Δ between the two stimulating electrodes. Finally the stimulating electrostatic pressure reads:

$$P(t) = P_1 \cos(2\pi ft) + P_2 \cos(2*2\pi ft + \varphi) \qquad (2)$$

where φ is the real phase shift experienced by the the jet surface: $\varphi = \phi - 2\pi f\Delta/U_o$. The ink-jet break-up is studied using a visualisation technique described elsewhere[4]. The microcomputer used to generate the electrode signals also triggers a strobe light (LED) which allows the observation of the magnified jet profile on a video display. The mean velocity U_o of the jet is determined from the relationship $U_o = \lambda f$ (λ the wavelength $\cong$ 3.3 mm). In order to observe closely the break-up of the jet, the formation and lifetime of the satellites, we introduce a variable phase shift between the electrode triggering signals and those of the LED. This allows to strobe the jet at different relative times, i.e. at different axial locations. The lifelengths of satellites are read on a digital display connected to the translation stage holding the nozzle, whereas their diameters are found from a shadow method using a slit of known dimensions[7]. The fluid used is a dyed glycerine-water mixture (65% glycerine) with viscosity $\eta \cong 17$ mPa.s, surface tension $T \cong 57 \cdot 10^{-3}$ N/m and mass density $\rho \cong 1168$ kg/m^3 at room temperature[4,8]. The presence of the dye allows to obtain a conductivity σ for the mixture of about 1.6 10^{-3} S/cm.

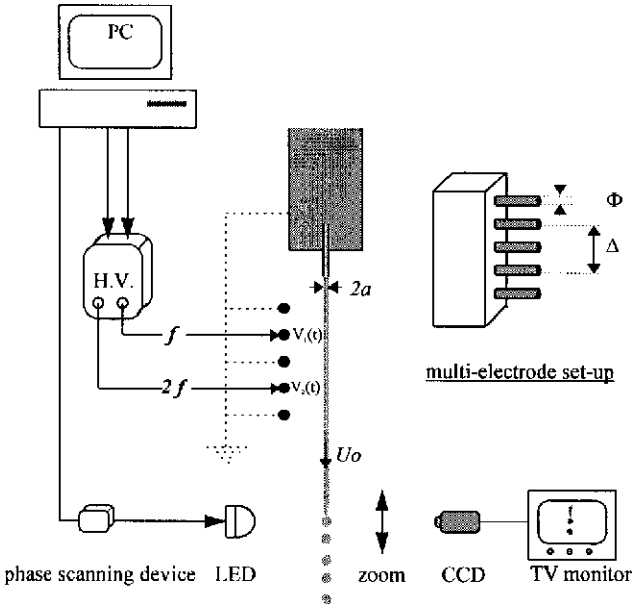

Figure 1. Schematic representation of the jet stimulation device

Different Régimes of Breakup

As noticed by Rezanka and Crowley[6], there are different régimes depending on both the ratio of the electrostatic pressures P_1/P_2 and the phase shift φ. For very small values of P_2/P_1 (<<1), the breakup is determined by the fundamental stimulating mode and there are 2 droplets per wavelength λ: one main drop and one large satellite (Figure 2a and bottom left corner of Figure 3). When the second mode is predominant (P_2/P_1>>1), there are 4 droplets per wavelength λ, corresponding to the mode 2*f*: 2 drops and 2 small satellites (Figure 2b and top right corner of Figure 3). For some intermediate values of P_2/P_1, we may expect 3 droplets. The region of particular interest in ink-jet printing is where only one drop is generated. It is therefore important to delineate the different modes of drop production in the map P_2/P_1 versus φ.

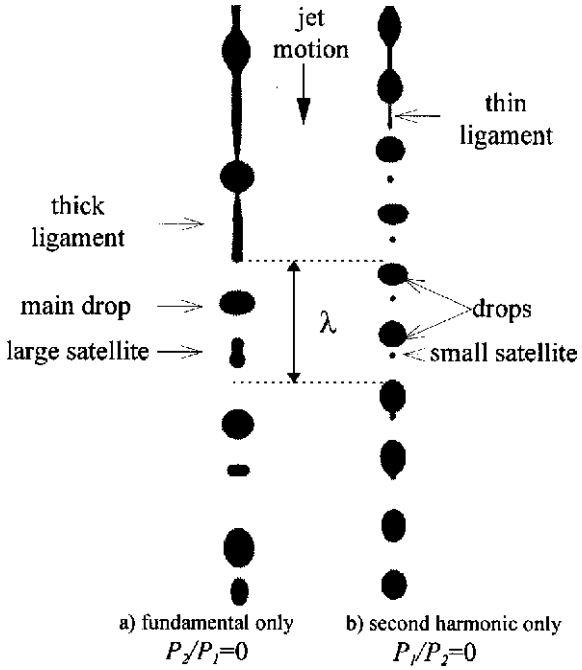

Figure 2. Jet break-up patterns

Such a map is given in Figure 3 for the wavenumber k = 0.400. It shows the various regions in the stimulation parameter plane leading to 1, 2, 3 or 4 droplets. Inserted in this figure, are photographs showing three wavelengths of the jet in the break-up area, in order to illustrate typical figures of jet deformation.

For φ = 300°, increasing P_2/P_1 results first in a large satellite which slows down until there is no separation from the main drop (no-satellite zone for $0.17 < P_2/P_1 < 0.29$ delineated by the bold line). This is the appropriate zone for ink-jet printing. For $P_2/P_1 > 0.29$ the ligament gives rise to a small satellite which coalesces with the following drop (slow satellite). At higher values of the pressure ratio, the deformation of the main drop becomes more and more marked until it splits into 2 drops of similar size ($P_2/P_1 > 4.9$). Finally for $P_2/P_1 > 5.7$, a micro-satellite (much smaller in size than the «small satellite» of Figure 2) appears in between the 2 drops (Figure 3). Note that this succession of régimes remains qualitatively similar for φ varying from 260° to 380°.

For φ =180°, the large satellite from slow becomes a fast one (coalescing with the main drop in front of it); at $P_2/P_1 = 0.3$ it tends to merge into the main drop but simultaneously a part of the ligament is stretched and breaks up leading to a small satellite. In this case we did not encounter a no-satellite zone as reported in Rezanka

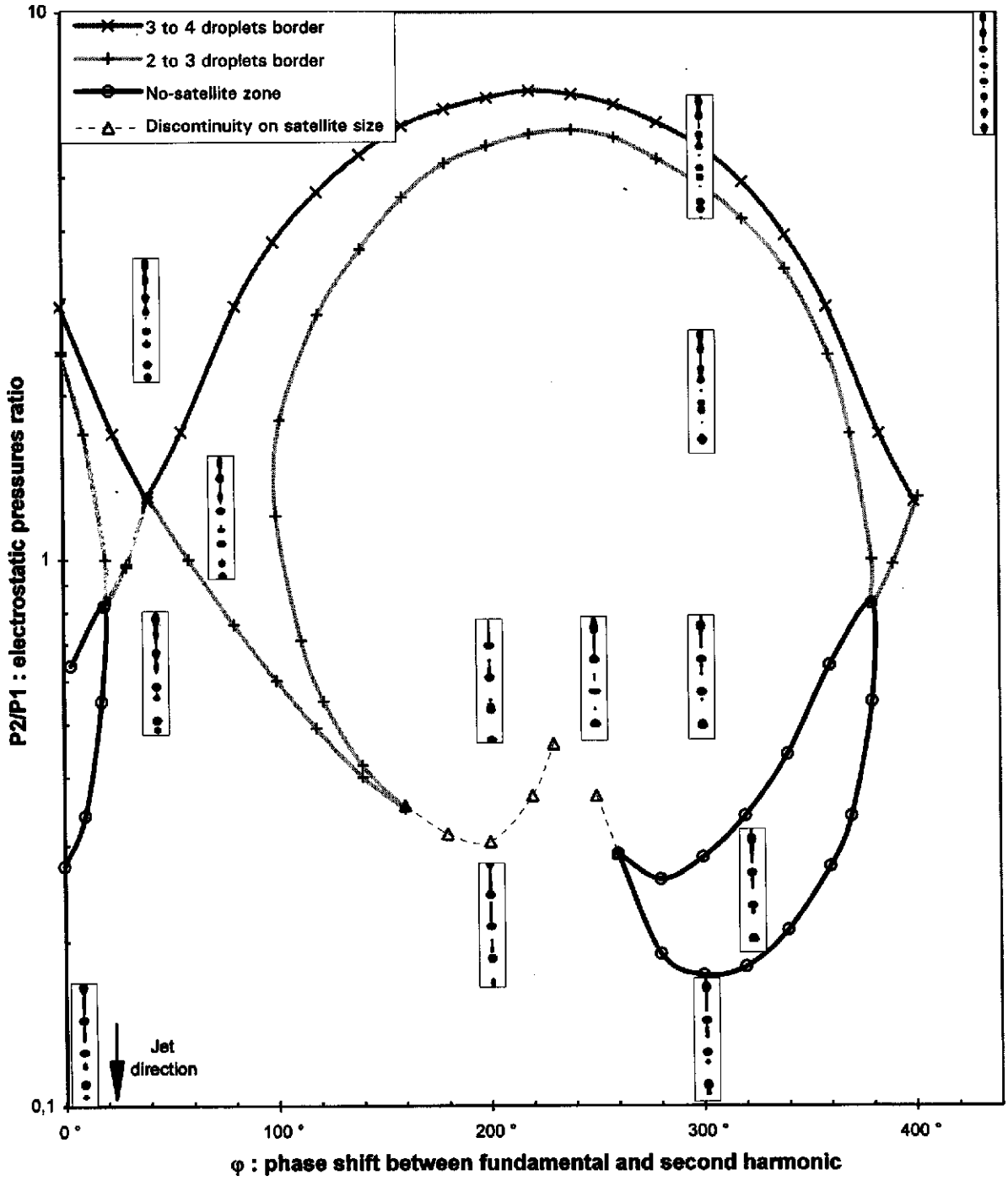

Figure 3. Break-up diagram at wave-number k = 0.400

and Crowley (see section IV). For P_2/P_1 increasing above 0.31, the phenomena are similar to those at φ = 300° except that the small satellite is at lower P_2/P_1 a fast one and at higher P_2/P_1 a slow one. The break-up occurs with the pear-like shape of the main drop facing the nozzle (this is the so called forward merging). The two dashed lines extending from φ = 160° to 230° and φ = 255° to 265° characterize a discontinuous change from the large satellite to the small one. At two critical points (φ = 230° and 255°) this discontinuity ceases. Indeed for the transition between both behaviours (φ = 250°), the large infinite satellite smoothly becomes a small one for P_2/P_1 = 0.6.

Outside the central loop zone, i.e. for 20° < φ < 100° the phenomena are simpler and there is a transition from 2 to 3 and then 4 droplets as P_2/P_1 is increased, except at the singular point (φ ≈ 40°) where one skips directly from 2 to 4 droplets.

Effect of Operating Conditions

Break-up Zones Without Satellites

As stated in the introduction, it is an essential requirement for technological reasons to obtain a drop formation devoid of satellites. In their work, Rezanka and Crowley[6] noticed two zones of no-satellite operating conditions for a wavenumber $k = 0.406$. In nearly similar conditions (wavenumber $k = 0.400$), we obtain the zone between 260° and 380°, but the zone near φ = 180° is absent (Figure 3).

This different behaviour may be due to the scale-up and/or the configuration of electrodes used in our experiments. Because of this, the electrical pressure is around one to two orders of magnitude smaller in our case compared to that of Rezanka and Crowley, although the electrical Euler number (ratio of electrical to dynamical pressure) turns out to be about of the same value. Nevertheless due to the scale-up, the hydrodynamics may not be exactly the same for the detachment and merging of much larger filaments than those usually found in ink-jet printing[9,10].

Another reason which can be invoked for the difference with Rezanka and Crowley's[6] results is that our wavenumber is slightly different from theirs. So, we have performed experiments at three other different wavenumbers ($k = 0.350$, $k = 0.450$, and $k = 0.437$). In the latter case (see Figure 4), we succeed in finding a no-satellite zone for the forward merging process (φ between 100° and 180°). The discrepancies with the observations of Rezanka & Crowley[6] lie in the shapes and the abscissae locations of the no-satellite zones. This value of $k = 0.437$ seems optimal in printing applications since the drop size is smaller, the break-up length shorter and moreover for $k = 0.350$ the no-satellite zone is absent whereas for $k = 0.450$ the second harmonic is no more amplified.

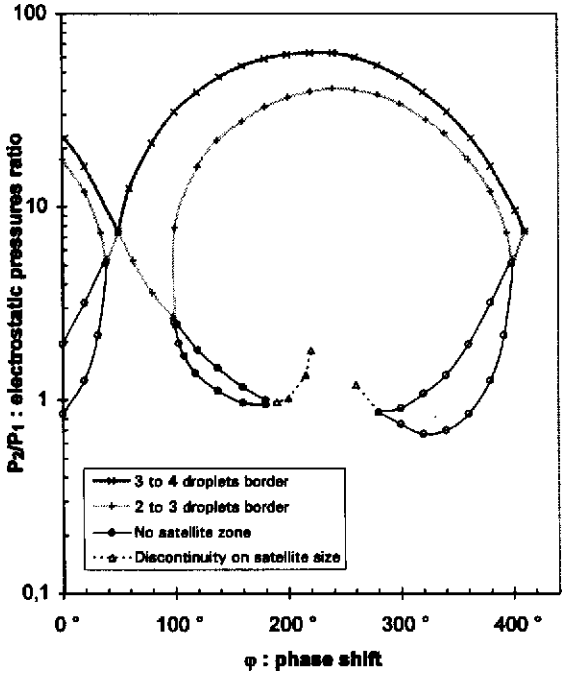

Figure 4. Break-up diagram at wave-number k = 0.437

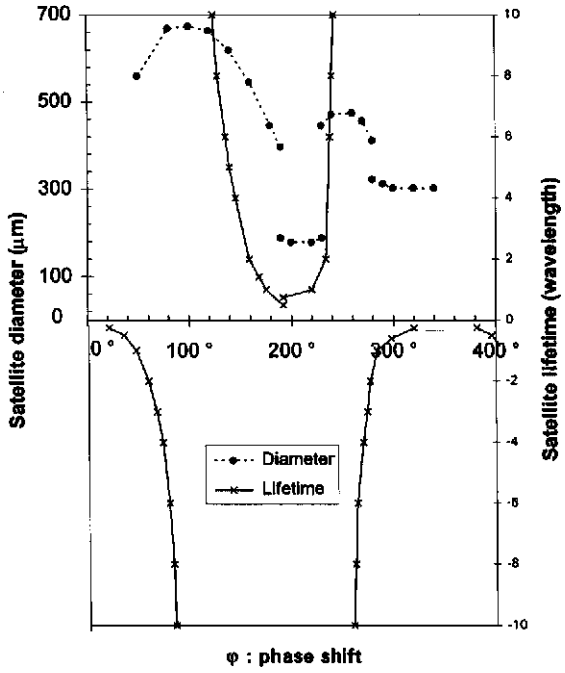

Figure 5. Satellite patterns for P2/P1=0.33 and k=0.4000

Lifetime and Size of Satellite Droplets

We also present in Figure 5 typical experiments performed at various phase shifts for fixed amplitude ratio $P_2/P_1 = 0.31$ and constant wavenumber k = 0.400. For φ = 0° we encounter the no-satellite zone delineated by the bold line of Figure 3. For increasing values of φ a very short life satellite is first noted at φ = 20°. The satellite lifetime given in wavelengths (positive lifetime is related to a fast satellite, negative lifetime to a slow one) begins to increase from φ = 40° upto φ = 100° (infinite satellite and maximal diameter). It then slowly decreases up to φ = 180°. At this point, as mentioned in section III there is creation of a small satellite with minimal lifetime. The creation process of the small satellite is first a separation on the aft side followed by some liquid being drained into the main front drop. This explains the sharp decrease in satellite diameter observed for φ = 190°. Diameter discontinuities found for the particular amplitude ratio investigated, reflect different break-up mechanisms. The smaller satellite diameters are found for 180°<φ<220° and 280°<φ<320° with the break-up occuring with mass transfer as stated above. The maxima in satellite diameters are for φ =100° and φ =260° where a double end pinch-off process without mass transfer takes place.

Conclusions

An experimental investigation of the break-up of an ink-jet submitted to harmonic EHD stimulation has been shown to lead to a variety of drop break-up patterns. We have determined the break-up maps for different wavenumbers as a function of both the electrostatic pressures ratio and the phase shift between the fundamental and the second harmonic of the stimulation signal. Several discrepancies appearing with the work of Resanka and Crowley have been noted and

explained. Moreover, other features of the jet break-up such as satellite sizes and lifetimes have also been considered in detail. This allows to define optimal operating conditions for ink-jet printers in terms of drop break-up.

Acknowledgements

We wish to thank the management of TOXOT Science & Applications for permission to publish this paper and especially Dr A. Dunand for helpful comments. We also thank the Centre National de la Recherche Scientifique (CNRS) for partially funding the study (contract CNRS/IMAJE No 50.9776). This study has also received partial financial support from the Ministère de la Recherche et de l'Enseignement Supérieur under grant No 92 P 0645. B. Barbet's PH. D. thesis work is performed under CIFRE/ANRT grant No 032/94.

References

1. G. L. Fillmore and D. C. Van Lokeren, *IEEE-IAS Conference Proceedings*, October 4-8, 1982.
2. A. Badea, A. Dunand, A. Soucemarianadin and C. Carrasso, *IS&T 9th Intl. Congress on Advances in Non Impact Printing Technologies*, pp. 256-259, 1993.
3. J. M. Crowley, *IEEE Transactions on Industry Applications*, **6**, pp. 973-976, 1986.
4. A. Spohn, P. Atten, A. Soucemarianadin and A. Dunand, *IS&T 9th Intl. Congress on Advances in Non Impact Printing Technologies*, pp. 294-297, 1993.
5. K. C. Chaudary and T. Maxworthy, *J. Fluid Mech*, vol. **96**, part 3, pp. 287-297, 1980.
6. I. Rezanka and J. M. Crowley, *Journal of Imaging Technology*, vol. **16**, no. 1, February 1990.
7. J. H. Xing, A. Boguslawski, A. Soucemarianadin, P. Atten and P. Attané, accepted for publication in *Exp. in Fluids*, 1995.
8. C. Bardeau, D. Fressard, P. Atten and B. Barbet, *IS&T 10th Intl. Congress on Advances in Non Impact Printing Technologies*, pp.439-433, 1994.
9. S. A. Curry and H. Portig, *IBM J. Res. Develop.*, pp. 10-20, January 1977.
10. P. Vassallo and N. Ashgriz, *Proc. R. Soc. Lond. A*, vol. **433**, pp. 269-286, 1991.